MODELING NON-UNIFORM-SEDIMENT FLUVIAL PROCESS BY CHARACTERISTICS METHOD

By Keh-Chia Yeh,[1] Associate Member, ASCE, Shian-Jang Li,[2] and Wen-Lin Chen[3]

ABSTRACT: This paper presents a numerical model based on a multimode characteristics method for fully coupled simulation of water and sediment movement in mobile-bed alluvial channels with nonuniform bed materials. Along with the characteristics, the temporal evolutions of flow depth and velocity, bed elevation, and bed-material composition of a well-defined river reach with proper boundary conditions can be simultaneously determined. From the results of the test runs, the proposed model provides useful information about the interactions among disturbance waves of different orders of magnitude and their influence on the formation of flow field, bed topography, and bed-material composition. Such information cannot be easily obtained from finite-difference methods.

INTRODUCTION

Alluvial rivers always evolve toward their dynamic equilibriums subject to upstream inflow, sediment discharges, and various human interventions such as watershed management, bed-material mining, dam construction, bridge pier construction, and channel regulation. River engineers are often faced with the challenge of predicting the effect of natural and unnatural disturbances on the channel equilibrium, and of proposing proper measures to mitigate undesirable consequences. To predict riverbed evolution, one generally resorts to physical modeling and/or numerical modeling. The latter is becoming more widely used due to its economy and flexibility in changing boundary and initial conditions of the problem.

Numerical modeling of mobile-bed evolution first appeared around two decades ago. Earlier, uncoupled models prevailed due to their computational simplicity and the large difference in magnitude of the celerities between water and bed-deformation waves. Recently, coupled models using finite-difference (FD) schemes, e.g., Rahuel et al. (1989), Holly and Rahuel (1990), and Correia et al. (1992), have been developed. Some of them incorporate newly proposed sediment-transport theories, e.g., nonequilibrium sediment transport and interaction between suspended load and bed load, to describe the complicated alluvial-river processes. In addition, models that adopt the method of characteristics (MOC) have also been proposed. The progress of model development based on the MOC is slower than that of the FD method. This is partly due to not knowing how to implement the MOC to alluvial rivers with nonuniform sediment.

However, the advantage of the MOC is that the physics behind the alluvial process can be well interpreted. The problem can be formulated as a set of hyperbolic partial differential equations, and the MOC is one of the most suitable methods to solve such a wave-type problem. Hence, the use of the MOC should still be attractive to researchers and for applications. De Vriend (1973) and Wu (1973) are among the early researchers trying to solve the uniform-sediment mobile-bed problems using the MOC. After years of endeavor, Lai (1991) developed a three-characteristic numerical model using the so-called multimode scheme to simulate coupled, unsteady, uniform-sediment alluvial-channel flow. In his model, three partial differential equations, i.e., the equations of continuity and motion for sediment-laden flow and the continuity equation of sediment transport, are first transformed into three pairs of characteristics and compatibility equations. Three unknowns, i.e., flow depth, velocity, and bed elevation, at each time step are then solved simultaneously. Lai (1991) concluded that numerical interpolation-stability versus extrapolation-instability relationships for the three-characteristic model are essentially the same as those for the two-characteristic model (i.e., fixed-bed cases). On numerical accuracy, Lai (1991) pointed out that the accuracy increases with a decrease in the size of spatial intervals and with an increase in the reachback number of the time domain.

Because natural alluvial rivers are composed of nonuniform bed materials, the three-characteristic MOC for solving uniform bed-material cases has its physical limitations. To improve these limitations, a numerical model based on the multimode MOC for the nonuniform sediment transport problems (herein called NMMOC model) is developed in this paper. Basic concepts

[1]Assoc. Prof., Dept. of Civ. Engrg., Nat. Chiao Tung Univ., Hsinchu, Taiwan, R.O.C.
[2]Former Grad. Student, Dept. of Civ. Engrg., Nat. Chiao Tung Univ., Hsinchu, Taiwan, R.O.C.
[3]Grad. Student, Dept. of Civ. Engrg., Nat. Chiao Tung Univ., Hsinchu, Taiwan, R.O.C.

Note. Discussion open until July 1, 1995. To extend the closing date one month, a written request must be filed with the ASCE Manager of Journals. The manuscript for this paper was submitted for review and possible publication on September 23, 1993. This paper is part of the ***Journal of Hydraulic Engineering***, Vol. 121, No. 2, February, 1995. ©ASCE, ISSN 0733-9429/95/0002-0159–0170/$2.00 + $.25 per page. Paper No. 7045.

of the NMMOC model are essentially adopted from the works by Yang et al. (1992) and Yeh et al. (1993). The NMMOC model can solve simultaneously ($N + 3$) pairs of characteristics and compatibility equations, with N being the number of different bed-material size fractions. Because of the introduction of N continuity equations for each size fraction of the bed materials, the numerical algorithm is more sophisticated than that proposed by Lai (1991).

In the following, the basic assumptions, mathematical formulation, solution algorithm, and test runs of the NMMOC model are reported. Simulation results indicate that the proposed model can clearly trace the bed deformation and change in bed-material composition.

GOVERNING EQUATIONS

Given the following conditions, a quite straight channel, a flow-resistance law valid for both steady and unsteady flows, an equilibrium suspended load capacity, no spatial-delay effects of bed-load transport (Bell and Sutherland 1983), constant mixing-layer thickness in the bed, and no armoring phenomenon during persistent degradation, then the governing one-dimensional unsteady equations for sediment-laden flow in a non-uniform-sediment alluvial channel without lateral inflows can be written as follows:

$$\frac{\partial z}{\partial t} + \frac{\partial h}{\partial t} + u\frac{\partial h}{\partial x} + \frac{A}{B}\frac{\partial u}{\partial x} + \frac{u}{B}\frac{\partial A}{\partial x}\bigg|_h = 0; \quad \frac{\partial u}{\partial t} + u\frac{\partial u}{\partial x} + g\frac{\partial h}{\partial x} + g\frac{\partial z}{\partial x} = -gS_f \tag{1, 2}$$

$$\frac{\partial z}{\partial t} + \frac{1}{(1 - p_r)B}\frac{\partial (q_s B)}{\partial x} = 0; \quad \frac{\partial P_{bi}}{\partial t} = -\frac{1}{a(1 - p_r)B}\left[\frac{\partial (q_{si} B)}{\partial x} - F_b \frac{\partial (q_s B)}{\partial x}\right]; \text{ for } i = 1, \ldots, N \tag{3, 4}$$

where z = bed elevation; h = flow depth; t = time; x = distance; u = flow velocity; A = flow area; B = channel width; $\partial A/\partial x|_h$ = the rate of change of A with respect to x when h is held constant; g = gravitational acceleration; S_f = friction slope; p_r = sediment porosity; q_s = sediment discharge in volume per unit width; P_{bi} = fraction of sediment in the ith size range, d_{si}, in the active layer; q_{si} = sediment discharge of ith size range per unit width; a = thickness of mixing layer; $F_b = P_{bi}$ in case of bed aggradation; and $F_b = P_{bio}$ in case of bed degradation, in which P_{bio} = fraction of sediment in the ith size range of the parent bed. Eqs. (1) and (2) are the continuity and momentum equations for sediment-laden flow, respectively. Eq. (3) is for conservation of bed material, and (4) is the sorting equation for each size fraction of sediment. Sediment transport relation can be stated as follows:

$$q_s = \sum_{i=1}^{N} q_{si} = \sum_{i=1}^{N} P_{bi} f_i(u, h, d_{si}, \ldots) \tag{5}$$

in which f_i = transport capacity of d_{si}, which is a function of flow intensity and sediment properties. In this study, the Engelund-Hansen formula (1967) is adopted

$$q_s = 0.05u^2 \left[\frac{d_{50}}{g(s_g - 1)}\right]^{1/2} \left[\frac{\gamma h S_f}{(\gamma_s - \gamma)d_{50}}\right]^{3/2} \tag{6}$$

in which s_g = specific gravity of the sediment; d_{50} = median particle size; and γ_s, γ = specific weights of sediment and water, respectively. The units used in (6) are in the English system. To obtain the respective sediment discharge of each particle size d_{si}, (6) is used to calculate the sediment discharge capacity f_i by replacing d_{50} with d_{si}. The total sediment discharge is then $\Sigma_{i=1}^{N} P_{bi} f_i$. Note that this estimation is not equal to that calculated directly from (6) using the representative d_{50} of the nonuniform bed material as originally proposed by Engelund and Hansen. Hence a correction factor, C_f, of the following form is used in the calculation of f_i:

$$C_f = \frac{q_s}{\sum_{i=1}^{N} P_{bi} f_i} = \frac{1}{d_{50}} \sum_{i=1}^{N} \frac{d_{si}}{P_{bi}} \tag{7}$$

Instead of being solved directly, (1)–(4) are transformed into ordinary differential equations.

TRANSFORMATION OF GOVERNING EQUATIONS

Using the notations $z_t = \partial z/\partial t$, $u_x = \partial u/\partial x$, . . . , $P_{bit} = \partial P_{bi}/\partial t$, etc., (1)–(4) can be expressed as follows:

$$J_i = P_{bit} + f_i' P_{bix} - \delta_i \sum_{j=1}^{N} f_j P_{bjx} + \bar{\psi}_i h_x + \bar{\omega}_i u_x + \gamma_i = 0; \qquad \text{for } i = 1, \ldots, N \tag{8}$$

$$J_{N+1} = z_t + h_t + uh_x + \frac{A}{B}u_x + \alpha = 0; \quad J_{N+2} = u_t + uu_x + gh_x + gS_f = 0 \tag{9, 10}$$

J. Hydraul. Eng. 1995.121:159-170.

$$J_{N+3} = z_i + a \sum_{j=1}^{N} f_i' P_{bi} + \frac{1}{p'} \psi h_i + \frac{1}{p'} \omega u_i + \beta = 0 \tag{11}$$

in which $\psi = \partial q_i/\partial h$; $\omega = \partial q_i/\partial u$; $\psi_i = \partial q_{si}/\partial h$; $\omega_i = \partial q_{si}/\partial u$; $p' = 1 - p_i$; $f_i' = f_i/(ap')$; $\delta_i = F_{bi}/(ap')$; $\bar{\psi}_i = (\psi_i - F_{bi}\psi)/(ap')$; $\bar{\omega}_i = (\omega_i - F_{bi}\omega)/(ap')$; $\gamma_i = (q_{si} - F_{bi}q_i)B_i/(ap'B)$; $\alpha = u/B(\partial A/\partial x)|_{h_i}$; and $\beta = q_i B_i/(p'B)$.

Combining (8)–(11) linearly with the constants $a_1, \ldots, a_{N+3}$ yields the following:

$$JS = a_1 J_1 + \cdots + a_N J_N + a_{N+1} J_{N+1} + a_{N+2} J_{N+2} + a_{N+3} J_{N+3} = 0 \tag{12}$$

After collecting related terms, (12) reduces to

$$JS = a_1 \frac{DP_{b1}}{Dt} + \cdots + a_N \frac{DP_{bN}}{Dt} + a_{N+1} \frac{Dh}{Dt} + a_{N+2} \frac{Du}{Dt} + (a_{N+1} + a_{N+3}) \frac{Dz}{Dt} + G = 0 \tag{13}$$

in which the total derivative $D(\ )/Dt = \partial(\ )/\partial t + [\partial(\ )/\partial x]\, dx/dt$ represents the differentiation in a given characteristic direction under the condition

$$\lambda = \frac{dx}{dt} = \frac{a_{N+3} f_i' a + a_i f_i' - f_i \sum_{j=1}^{N} a_j \delta_j}{a_i}; \quad \text{for } i = 1, \ldots, N \tag{14a}$$

$$\lambda = \frac{dx}{dt} = \frac{\sum_{j=1}^{N} a_j \bar{\psi}_j + a_{N+1} u + a_{N+2} g + a_{N+3} \dfrac{\psi}{p'}}{a_{N+1}} \tag{14b}$$

$$\lambda = \frac{dx}{dt} = \frac{\sum_{j=1}^{N} a_j \bar{\omega}_i + a_{N+1} \dfrac{A}{B} + a_{N+2} u + a_{N+3} \dfrac{\omega}{p'}}{a_{N+2}} \tag{14c}$$

$$\lambda = \frac{dx}{dt} = \frac{a_{N+2} g}{a_{N+1} + a_{N+3}} \tag{14d}$$

with λ = characteristic value or eigenvalue; and

$$G = a_1 \gamma_1 + \cdots + a_N \gamma_N + a_{N+1} \alpha + a_{N+2} g S_f + a_{N+3} \beta \tag{15}$$

Eqs. (14) and (13) are the characteristic and the compatibility equations corresponding to the original partial differential equations. Rearranging (14) yields a homogeneous system of $(N + 3)$ linear equations. By the row operation, the problem of solving the system of equations reduces to an eigenvalue problem. According to Cramer's theorem, it has a nontrivial solution of unknown column vector $[a_1, \ldots, a_{N+3}]^T$ (called eigenvector) if and only if the corresponding determinant of the coefficient matrix is zero. This leads to a polynomial of $(N + 3)$th degree in eigenvalue λ. Hence, the $(N + 3)$ eigenvalues can be obtained from the polynomial. Because the degree of the polynomial in λ is larger than three, the roots (or eigenvalues), in general, have to be solved numerically.

From the definition in (14), the eigenvalues represent the celerities of the $(N + 3)$ waves associated with liquid and solid particle disturbances in a channel. Given the eigenvalues, integration of (14) yields $(N + 3)$ trajectories of disturbances associated with water and sediment. These trajectories are called the characteristics. Interpretation of fluvial process along the characteristics is the central concept of the MOC.

Two of the $(N + 3)$ characteristics are related to water-surface disturbances, and the remaining characteristics correspond to disturbances of bed deformation and composition variation in the mixing layer. It can be shown analytically or numerically that one of the remaining $(N + 1)$ eigenvalues is always zero because the sum of the N sorting equations for size classes in the mixing layer is a global expression of conversation of bed material, i.e., (3). Bed-deformation disturbance in a non-uniform-sediment river bed is always accompanied by the sediment composition change in the mixing layer. For a given flow intensity, the smallest sediment is the easiest one among all particle sizes to be detached from the bed. Hence, the celerity of bed deformation is the same as that of fraction-variation of the smallest sediment in the mixing layer. After excluding eigenvalues of the two water-surface disturbances, bed-deformation disturbance, and zero, $(N - 1)$ eigenvalues remain having a one-to-one correspondence with the fraction-variation disturbances of the remaining $(N - 1)$ larger particles with the larger absolute eigenvalues corresponding to the propagating celerities of the smaller particles.

When the channel is composed of uniform bed material, i.e., $N = 1$, (4) is redundant. Under such circumstances, only three equations, i.e., (1)–(3), are required to solve for flow depth, velocity, and bed elevation. Then, three distinct eigenvalues (or celerities) associated with the water-surface and bed-deformation disturbances can be obtained from the characteristics method.

ALGORITHM OF NMMOC MODEL

Discretization

Eqs. (13) and (14) can be discretized in the finite-difference form and solved numerically. Consider an x-t rectangular grid system in a plane, in which time intervals Δt are set equal, and distance intervals Δx_j are not necessarily equal (Fig. 1). At any interior grid point p at (x_j, t_{k+1}), there are $(N + 3)$ characteristic curves passing through it. To solve for the $(N + 3)$ unknown variables, i.e., $P_{b1}, P_{b2}, \ldots, P_{bN}, h, u$, and z, at point p, the governing equations [(13) and (14)] are discretized as follows:

$$x_p - x_i = \lambda_{ip}(t_p - t_i); \quad \text{for } i = 1, \ldots, N + 3 \tag{16}$$

$$a_{1,ip}(P_{b1p} - P_{b1i}) + \cdots + a_{N,ip}(P_{bNp} - P_{bNi}) + a_{N+1,ip}(h_p - h_i) + a_{N+2,ip}(u_p - u_i) + (a_{N+1,ip} + a_{N+3,ip})(z_p - z_i) + G_{ip}(t_p - t_i) = 0; \quad \text{for } i = 1, \ldots, N + 3 \tag{17}$$

in which a single or triple subscript = a grid or interception point; and a double subscript = a curve segment of a given characteristic. Let ϕ'_{ip} = a general representation of quantities λ_{ip}, $a_{1,ip}, \ldots, a_{N+3,ip}$, and G_{ip}, which are functions of $(N + 3)$ variables at point p and i. Then ϕ'_{ip} can be approximated as follows:

$$\phi'_{ip} = \theta\phi'_i + (1 - \theta)\phi'_p \tag{18}$$

in which θ = weighting factor. The location of the interception point i can be determined if λ_{ip} is given. Let ϕ_i = a general representation of the $(N + 3)$ variables at i. The expression of ϕ_i in terms of the ϕ values at its two adjacent grid points using the multimode scheme (see Fig. 1) is

$$\phi_1 = \xi_1\phi_{j-1}^{k} + (1 - \xi_1)\phi_{j-1}^{k+1} \quad \text{for implicit scheme} \tag{19a}$$

$$\phi_2 = \eta_1\phi_{j-1}^{k} + (1 - \eta_1)\phi_j^{k} \quad \text{for explicit scheme} \tag{19b}$$

$$\phi_3 = \xi_2\phi_{j-1}^{k-m} + (1 - \xi_2)\phi_{j-1}^{k+1-m} \quad \text{for temporal reachback scheme} \tag{19c}$$

$$\phi_4 = \eta_2\phi_{j-1}^{k+1-M} + (1 - \eta_2)\phi_j^{k+1-M} \quad \text{for spatial reachback scheme} \tag{19d}$$

in which m = reachback number; M = allowed maximum reachback number; $\xi_{1,2}$ = temporal-interpolation factor; and $\eta_{1,2}$ = spatial-interpolation factor. These interpolation factors can be expressed as follows:

$$\xi_1 = \frac{\Delta x_j/\Delta t}{\left(\frac{dx}{dt}\right)_{1p}} = \frac{r_j}{\lambda_{1p}}; \quad m + \xi_2 = \frac{r_j}{\lambda_{3p}}; \quad \eta_1 = \frac{r_j}{\lambda_{2p}}; \quad \eta_2 = \frac{M\frac{\Delta x_j}{\Delta t}}{\left(\frac{dx}{dt}\right)_{4p}} = M\frac{r_j}{\lambda_{4p}} \tag{20a-d}$$

Substituting (18)–(20) into (17) yields the following:

$$F_i(\phi_{j-1}^{k+1}, \phi_j^{k+1}, \phi_{j+1}^{k+1}) = 0; \quad \text{for } i = 1, \ldots, N + 3 \tag{21}$$

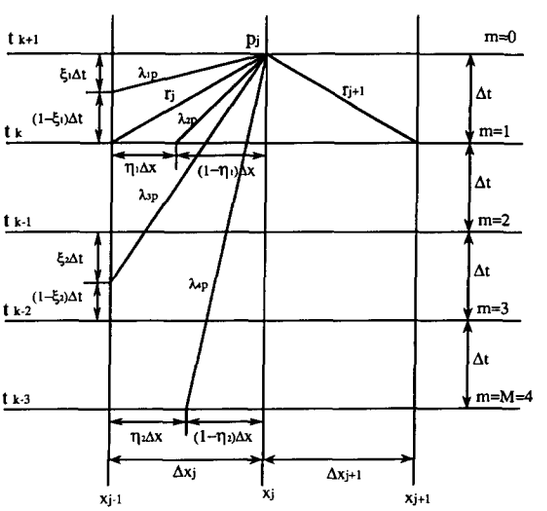

FIG. 1. Schematic Sketch of NMMOC

Boundary Conditions

Besides the requirement of the initial steady-state condition for the entire domain, boundary conditions which are related to characteristics or eigenvalues, are also needed in the model. For the case of uniform-sediment flow, which is a special case of non-uniform-sediment flow, Lai (1991) has shown analytically that the multiplication of the three distinct real eigenvalues is negative and, consequently, two of them should be positive. When the flow is supercritical, the two eigenvalues corresponding to the celerities of water-surface disturbances are positive (i.e., both disturbances propagate downstream). On the other hand, one of the water-surface disturbances is positive and the other is negative when the flow is subcritical. The eigenvalue representing the celerity of the bed deformation, therefore, is positive or negative depending on the flow being subcritical or supercritical. However, it is analytically impossible to determine the sign of every eigenvalue for the case of non-uniform-sediment flow with N different particle sizes. Because the celerity of bed deformation is the same as that of fraction variation of the smallest particle in the mixing layer and the smaller celerities for the remaining larger particles, it is intuitive that the N fraction-variation celerities have the same sign as that of the bed deformation. This intuition is verified from the numerical solution of the N fraction-variation eigenvalues in the study.

Based on this reasoning, one characteristic (upstream propagating water-surface disturbance wave) and $(N + 2)$ characteristics (one for the downstream propagating water-surface disturbance wave and the rest for the bed deformation and fraction-variation waves) at upstream and downstream boundaries, respectively, are available for the subcritical-flow condition. Therefore, $(N + 3)$ boundary conditions [$(N + 2)$ at the upstream boundary and one at the downstream boundary] are required to solve the problem under the sub-critical-flow condition. The characteristics at the boundaries and the required boundary conditions for the super-critical-flow condition can be obtained in a similar way.

There are several possible combinations of upstream and downstream boundary conditions. One such possibility for the subcritical flow is that water discharge and sediment composition and discharge are given as a function of time at the upstream boundary, and a depth and water discharge relationship at the downstream boundary. The required boundary conditions can be stated as follows:

$$F_i(\phi_b^{k+1}) = 0 \tag{22}$$

in which the subscript b denotes upstream or downstream boundary of a channel.

Solution

For an alluvial channel consisting of L subreaches, there are $(L + 1)(N + 3)$ unknowns to be solved at any time step. Combining (21) and (22) yields a set of $(L + 1)(N + 3)$ linear equations with $(L + 1)(N + 3)$ unknowns, which can be expressed as a block-diagonal matrix system of the following form:

$$\begin{bmatrix} \mathbf{D}_0 & \mathbf{R}_0 & & & & & & \\ \mathbf{L}_1 & \mathbf{D}_1 & \mathbf{R}_1 & & & & & \\ & \cdots & & & & & & \\ & & \mathbf{L}_j & \mathbf{D}_j & \mathbf{R}_j & & & \\ & & & \cdots & & & & \\ & & & & \mathbf{L}_{L-1} & \mathbf{D}_{L-1} & \mathbf{R}_{L-1} & \\ & & & & & \mathbf{L}_L & \mathbf{D}_L & \end{bmatrix} \begin{bmatrix} \mathbf{X}_0 \\ \mathbf{X}_1 \\ \cdots \\ \mathbf{X}_j \\ \cdots \\ \mathbf{X}_{L-1} \\ \mathbf{X}_L \end{bmatrix} = \begin{bmatrix} \mathbf{C}_0 \\ \mathbf{C}_1 \\ \cdots \\ \mathbf{C}_j \\ \cdots \\ \mathbf{C}_{L-1} \\ \mathbf{C}_L \end{bmatrix} \tag{23}$$

Note that the elements in the left-hand side matrix of (23) are $(N + 3)(N + 3)$ matrices. Using subcritical-flow condition as an example, $\mathbf{D}_0$, $\mathbf{R}_0$ = coefficient matrices associated with $(N + 2)$ upstream boundary conditions and one upstream propagating characteristic, respectively; $\mathbf{L}_j$, $\mathbf{D}_j$, $\mathbf{R}_j$ = coefficient matrices corresponding to $(N + 3)$ compatibility equations; $\mathbf{L}_L$, $\mathbf{D}_L$ = coefficient matrices associated with one downstream boundary condition and $(N + 2)$ downstream propagating characteristics, respectively; $\mathbf{X}_j$ = column vector of $(N + 3)$ unknowns at section j; and $\mathbf{C}_j$ = column vector of $(N + 3)$ constants at section j. Eq. (23) can be solved using the Thomas algorithm (e.g., Anderson et al. 1984) together with the lower-triangular and upper-triangular (LU) matrices decomposition technique [e.g., Gerald and Wheatley (1989)]. Because the coefficient matrix is nonsingular and the column vector of constants is nonzero, the solution is unique and nontrivial. The analyses on numerical stability and accuracy for the three-characteristic case has been done by Lai (1991), whose conclusions can be extended to the case of $(N + 3)$ distinct characteristics (Chen 1994; Lai 1994).

MODEL TEST AND COMMENTS

To examine the capability of the proposed NMMOC model to simulate non-uniform-sediment mobile-bed hydraulics, several tests were performed. The hypothetical river reach for the tests

J. Hydraul. Eng. 1995.121:159-170.

was 2.5 km long with a rectangular section 400 m in width. The space step used, Δx, was 100 m. The reason behind choosing such a short river length and Δx was to investigate the propagating speeds of bed deformation and fraction variation of bed material, which are much slower than those associated with water-surface disturbances. The slope of the initial river bed was 0.0002. Manning's n of 0.03 was adopted. A constant water discharge of 200 m^3/s with a duration of 90 days was assumed for the case of long-term steady flow. For the case of unsteady flow, water discharge at the upstream boundary increased linearly from 200 m^3/s to a peak of 3,000 m^3/s in 1.5 days and then decreased linearly back to 200 m^3/s in another 1.5 days. Uniform-flow condition was assumed at the downstream boundary for both steady and unsteady flows. Two sediment size classes were considered, i.e., $N = 2$, in all the tests. There were three initial bed compositions for the smaller size class ($d_{s1} = 0.125$ mm) and the larger size class ($d_{s2} = 1$ mm). In case 1, 50% of the bed material was d_{s1} and 50% was d_{s2} ($P_{b1} = 0.5$ and $P_{b2} = 0.5$); in case 2, it was 75% d_{s1} and 25% d_{s2} ($P_{b1} = 0.75$ and $P_{b2} = 0.25$); and in case 3, it was 25% d_{s1} and 75% d_{s2} ($P_{b1} = 0.25$ and $P_{b2} = 0.75$). The mixing-layer thickness for steady and unsteady flows was set as 0.2 m and 0.5 m, respectively. The upstream input sediment discharge, with composition the same as that of the initial bed, serves as an upstream boundary condition. For simplicity, the size fractions of the mixing layer at the upstream boundary were assumed to be constant during the simulation and served as N upstream boundary conditions. The allowed maximum reachback number, M, equaled one in all the tests.

Steady Flow

Due to its similarity, only the results of case 1 ($P_{b1} = 0.5$ and $P_{b2} = 0.5$) are presented here. The loading ratio (LR) is defined as the upstream imposed sediment discharge divided by

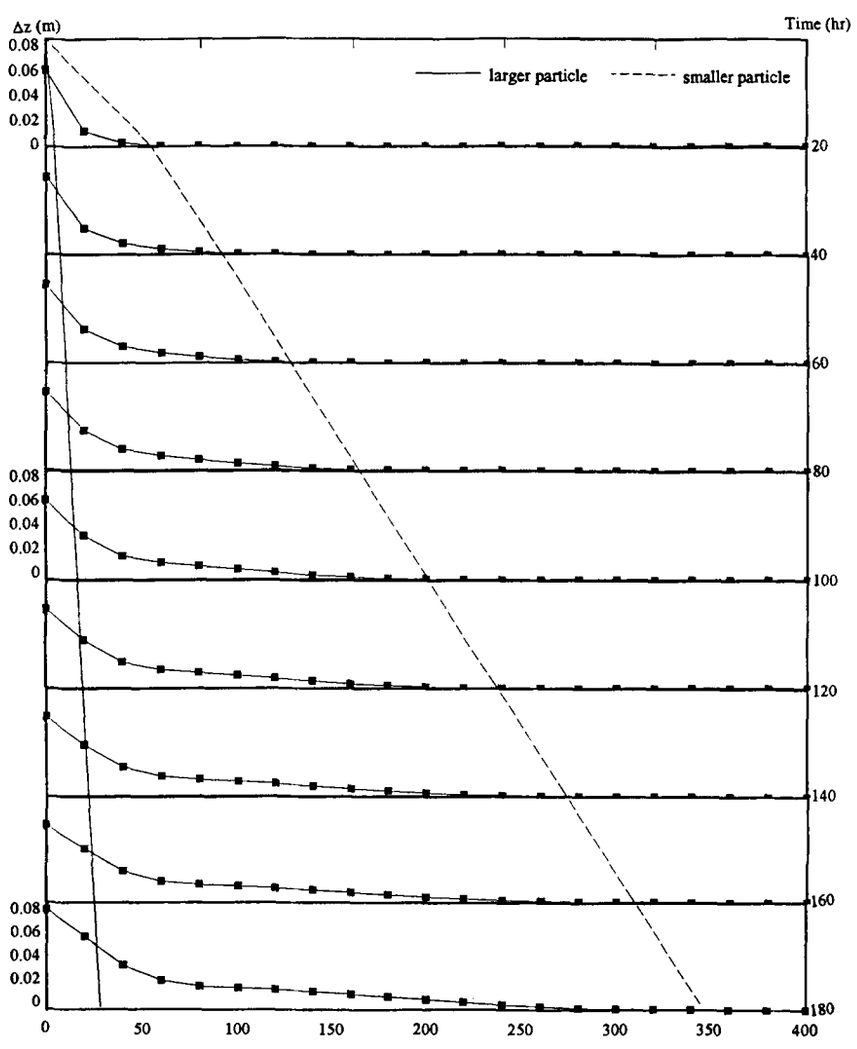

FIG. 2. Propagation of Wave Fronts for Bed Deformation and Composition Variations of Particles under Steady-Flow Condition with LR = 1.5

J. Hydraul. Eng. 1995.121:159-170.

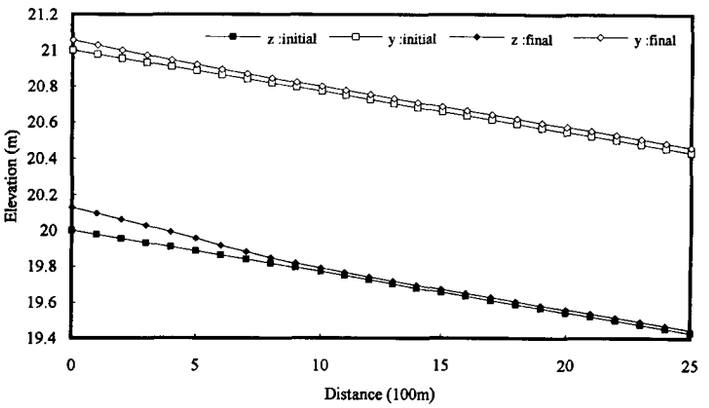

FIG. 3. Spatial Evolutions of Water-Surface and Bed Elevations under Steady-Flow Condition with LR = 1.5

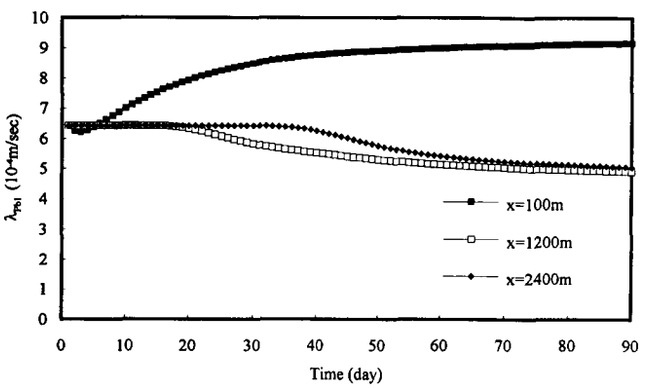

FIG. 4. Temporal Evolutions of λ_{Pb1} at Different Locations under Steady-Flow Condition with LR = 1.5

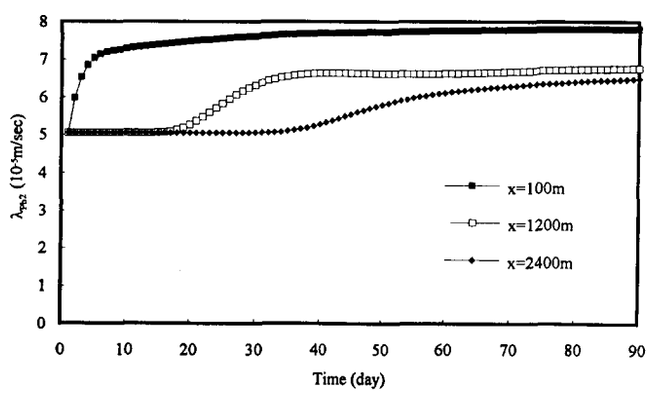

FIG. 5. Temporal Evolutions of λ_{Pb2} at Different Locations under Steady-Flow Condition with LR = 1.5

sediment transport capacity under the given water discharge and size fraction of bed material at the upstream boundary. When LR is larger than one, the river bed will aggrade; when LR is less than one, it will degrade.

Under the condition of LR = 1.5, Fig. 2 shows propagations of wave fronts of bed deformation (represented by bed-level change, Δz), and size-fraction variations of smaller and larger particles during the first 180 hr of the simulation. The fact that the celerity of bed deformation essentially coincides with that of the fraction variation of the smaller particle is valid. Bed-level change near the front is so small that it is difficult to discern from the figure as time goes on. The wave front of the larger particle falls far behind that of the smaller particle. Fig. 3 shows the initial and final (t = 90 days) bed profiles and water-surface elevation along the channel. The tendency of aggradation of the channel bed was correctly simulated by the proposed model. Figs. 4–7 further show the relationships among celerities of fraction variations of particles (λ_{Pb1} and λ_{Pb2}), Δz, and the mean particle size (d_m) in the mixing layer. In the initial equilibrium state, λ_{Pb1} (6.4×10^{-4} m/s) and λ_{Pb2} (5×10^{-5} m/s) are constant along the entire reach. Due to the

J. Hydraul. Eng. 1995.121:159-170.

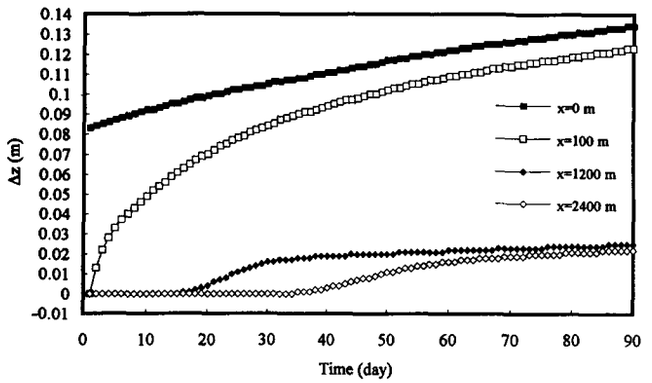

FIG. 6. Temporal Evolutions of Bed-Level Changes under Steady-Flow Condition with LR = 1.5

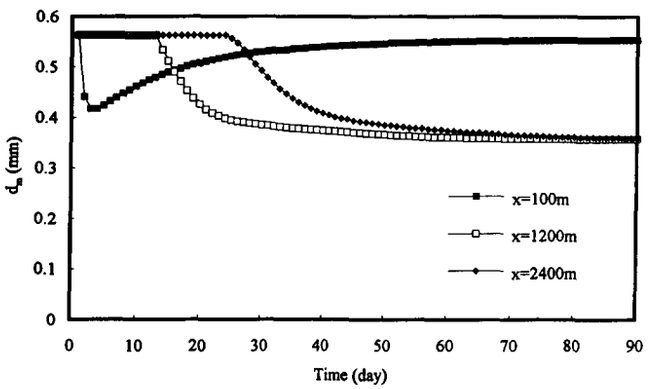

FIG. 7. Temporal Evolutions of Mean Particle Size in Mixing Layer under Steady-Flow Condition with LR = 1.5

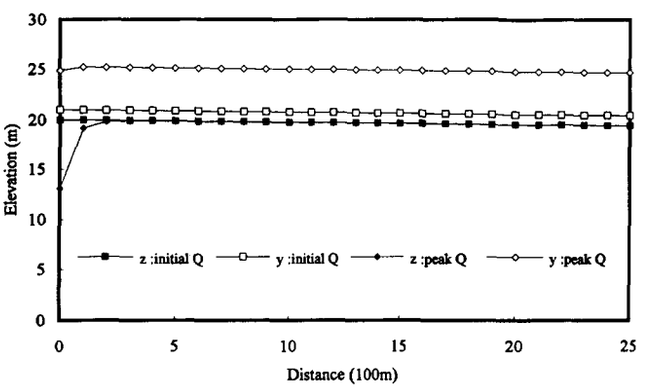

FIG. 8. Spatial Evolutions of Water-Surface and Bed Elevation at Initial Time and Time of Peak Discharge

overloading of imposed sediment discharge at the upstream boundary, equilibrium state no longer exists, and this can be detected by the change of λ_{Pb1}. When the characteristic associated with the new value of λ_{Pb1} reaches a specific section, the bed level, λ_{Pb2}, and d_m in the mixing layer at that section change accordingly. Aggradation of the channel bed causes decrease of d_m, which can be seen in Fig. 7. Comparing Figs. 5 and 6, one finds that λ_{Pb1} is approximately one-order-of-magnitude larger than λ_{Pb2}.

For the case of LR = 0.5, i.e., underloading of imposed sediment at the upstream boundary, the phenomena of channel-bed degradation, increase of d_m, and decrease of λ_{Pb1} and λ_{Pb2} were observed but not shown here. Tests on the effect of using different time steps (Δt = 1, 1.5, and 3 days) were also made for both overloading and underloading conditions. The simulation results were not sensitive to the choice of Δt.

Unsteady Flow

The loading ratio can be regarded as unity because the upstream inflow sediment discharge is calculated based on the bed-material composition and the flow intensity at any given time

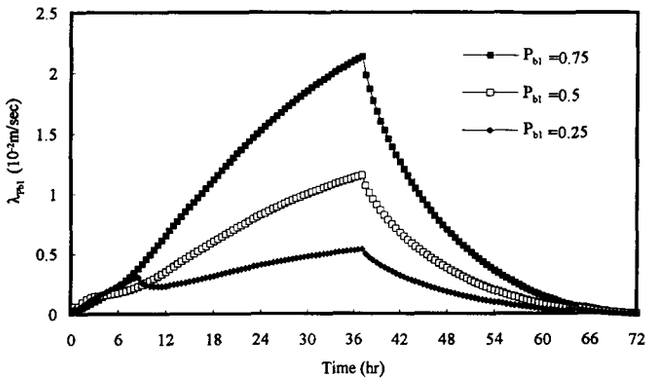

FIG. 9. Temporal Evolutions of λ_{Pb1} for Different Compositions under Un-Steady-Flow Condition at x = 100 m

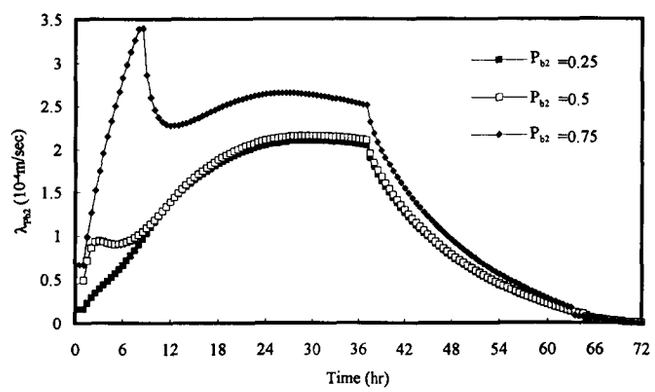

FIG. 10. Temporal Evolutions of λ_{Pb2} for Different Compositions under Un-Steady-Flow Condition at x = 100 m

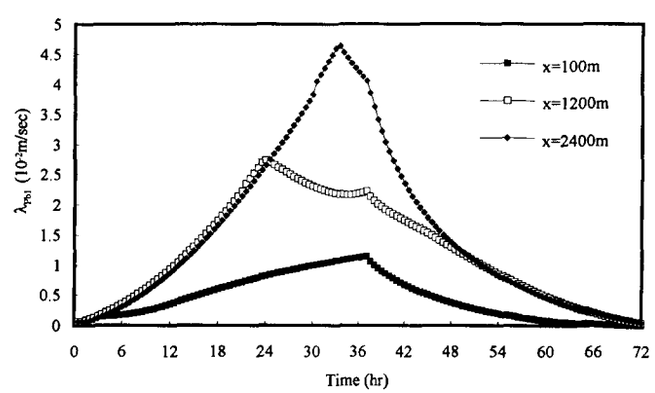

FIG. 11. Temporal Evolutions of λ_{Pb1} at Different Locations under Un-Steady-Flow Condition

step. The bed and water-surface elevations for case 1 at t = 36 hr is plotted in Fig. 8, from which significant change of bed and flow depth near the upstream boundary compared with the initial ones can be observed. The constant increase in inflow discharge, associated with the increase in sediment discharge on the rising limb of the unsteady hydrograph, results in local scour near the upstream boundary of the channel due to sediment continuity.

To examine the effect of sediment composition on the propagation of fraction-variation waves of particles, three compositions of sediment mixture mentioned previously were used. Figs. 9 and 10 show the variations of λ_{Pb1} and λ_{Pb2} at x = 100 m. Case 2 has the smallest value of d_m at the beginning and, consequently, has the largest magnitude of variation in λ_{Pb1} under the same inflow water discharge. Hence, the range of occurring bed deformation for case 2 is the largest for the same time level. The occurrence of the two peaks for λ_{Pb1} and λ_{Pb2}, as shown in Figs. 9 and 10, might be due to the effect of the nonlinear relationship among sediment discharge, flow intensity, and sediment properties, i.e., the sediment-transport formula.

Time evolutions of λ_{Pb1} and λ_{Pb2} at different sections for case 1 are shown in Figs. 11 and 12.

J. Hydraul. Eng. 1995.121:159-170.

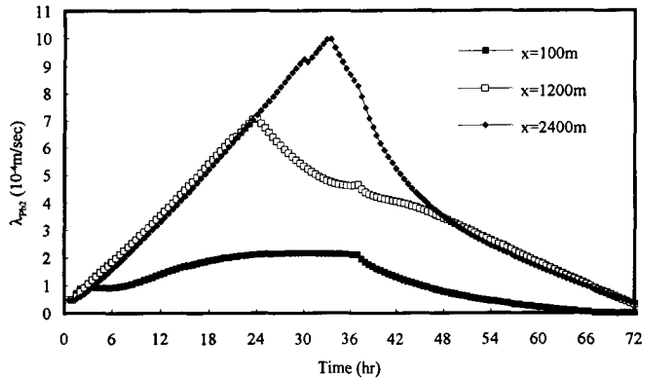

FIG. 12. Temporal Evolutions of λ_{Pb2} at Different Locations under Un-Steady-Flow Condition

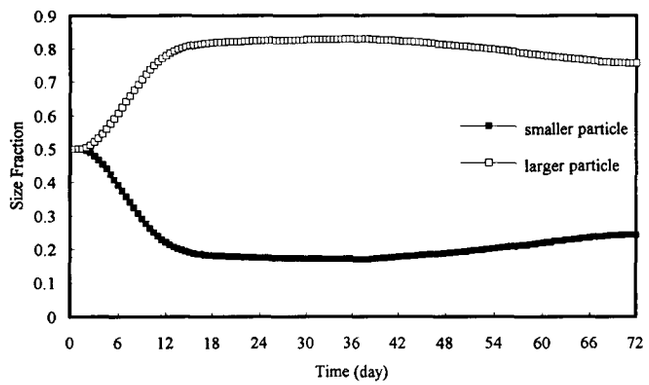

FIG. 13. Temporal Evolutions of Size Fractions under Un-Steady-Flow Condition at x = 100 m

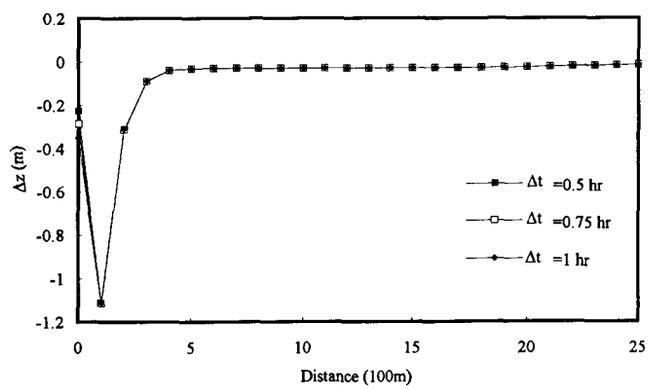

FIG. 14. Simulated Bed-Level Changes Using Different Δts under Un-Steady-Flow Condition

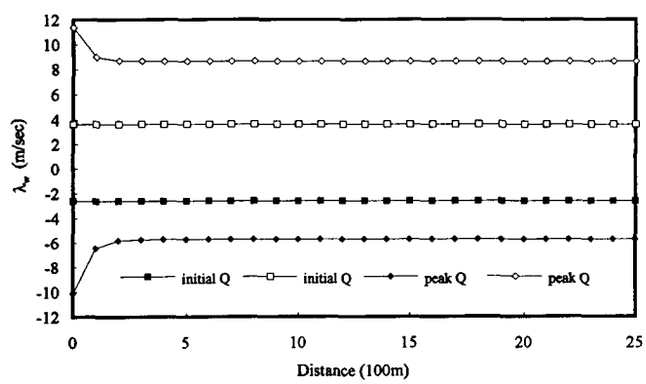

FIG. 15. Spatial Evolutions of λ_w at Initial Time and Time of Peak Discharge

It is interesting that the peaks of λ_{Pb1} and λ_{Pb2} at $x = 1{,}200$ m occur before the peak of inflow water discharge (occurring at $t = 36$ hr). The peak of λ_{Pb1} at $x = 100$ m is the smallest one due to the existence of a significant local scour near the upstream boundary (see Fig. 8). Peaks of λ_{Pb1} and λ_{Pb2} at different locations occur before or after the peak of water discharge and have no consistent trend. This might be attributed to the complicated nonlinearity of the problem, and further research is required. The temporal evolutions of size fractions for smaller and larger particles at $x = 100$ m are plotted in Fig. 13. It can be observed that d_m increases during the passage of the unsteady-flow hydrograph.

Different time steps ($\Delta t = 0.5$, 0.75, and 1 hr) were also used for the model stability test. From Fig. 14, the simulated results of bed-level change for case 1 are not sensitive to the choice of Δt. A comparison of Figs. 8 and 14 indicates that the local scour shifts a little from upstream boundary to the downstream reach after the passage of the unsteady-flow hydrograph. Celerities (λ_w) of the two characteristics associated with water-surface disturbances for case 1 at $t = 0$ and 36 hr, respectively, are plotted in Fig. 15. The negative values of λ_w represent waves propagating upstream. Comparing Figs. 15 and 11, λ_w is 10^3–10^4 times larger than λ_{Pb1}. This indicates that using uncoupled mobile-bed model will not result in losing much accuracy of the solution.

CONCLUSIONS

A new numerical model (NMMOC model) that extends the multimode characteristics method to model non-uniform-sediment alluvial-river hydraulics is described in this paper. In the model, original water continuity, momentum equations, and the bed-material continuity equation, together with N bed-material sorting equations, constitute $(N + 3)$ pairs of characteristic and compatibility equations. The $(N + 3)$ characteristic equations were used to find the $(N + 3)$ eigenvalues that represent wave celerities of disturbances. When N is greater than one, eigenvalues could be obtained numerically. One of the $(N + 3)$ eigenvalues is always zero due to the redundancy in the characteristic equations. The two largest absolute eigenvalues correspond to the celerities of water-surface disturbances. The third largest absolute value represents the celerity of bed deformation or fraction variation of the smallest particle in the mixing layer. The rest $(N - 1)$ eigenvalues correspond to $(N - 1)$ particles excluding the smallest one. Substituting $(N + 3)$ eigenvectors associated with the obtained $(N + 3)$ eigenvalues into the compatibility equations, the dependent variables such as flow depth and velocity, bed elevation, and bed-material composition can be solved. Iterations continue until the required accuracy of the solution is attained.

For model test, two particle sizes ($N = 2$) with different combinations of composition were considered. Furthermore, the temporal evolutions of eigenvalues associated with the propagations of fraction variation of the two particle sizes, with overload/underload of sediment, under steady- and un-steady-flow conditions were examined. Results show that for a nonequilibrium disturbance imposing at the upstream boundary of a reach the propagating speed of the bed deformation is determined by the magnitude of eigenvalue λ_{Pb1} of the smaller particle. Such information cannot be easily obtained by using the finite-difference method. The flow field changes due to bed deformation and boundary conditions that, in turn, affect the magnitude of λ_{Pb1} and the consequent bed deformation. The interactions among flow field, bed topography, and sediment composition, linked by the variation of λ_{Pb1}, continue towards a new equilibrium state. When the new equilibrium state is reached, λ_{Pb1} will approach a new constant value at a given section of the reach. From the simulation runs, the magnitude of λ_{Pb1} was found to be very small in comparison with that associated with water-surface disturbance. This might support the premise in the uncoupled models that the use of fixed-bed assumption in the phase of flow computation is acceptable in practical applications.

In the present NMMOC model, several assumptions (no armoring phenomenon, constant mixing-layer thickness, etc.) were made in the governing equations of alluvial-river flows. Further research is needed to account for these phenomena so that the proposed model can be applied to practical problems. Despite the above mentioned limitations, the proposed model provides important information that leads to better understanding of the complicated processes involving interactions among nonuniform sediments, bed topography, and flow field.

ACKNOWLEDGMENTS

This research is supported by the National Science Council of the Republic of China, under grant No. NSC81-0410-E009-18. Special thanks are due to J. C. Yang, C. M. Wu, and C. Lai for their invaluable discussions during the course of this study.

APPENDIX I. REFERENCES

Anderson, D. A., Tannehill, J. C., and Pletcher, R. H. (1984). *Computational fluid mechanics and heat transfer*. Hemisphere Publishing Corp., New York, N.Y.

Bell, R. G., and Sutherland, A. J. (1983). "Non-equilibrium bedload transport by steady flow." *J. Hydr. Engrg.*, ASCE, 109(3), 351–367.
Chen, W. L. (1994). "A study on channel aggradation using multimode characteristics method." MS thesis, Nat. Chiao Tung Univ., Hsinchu, Taiwan, R.O.C. (in Chinese).
Correia, L. R. P., Krishnappan, G., and Graf, W. H. (1992). "Fully coupled unsteady mobile boundary flow model." *J. Hydr. Engrg.*, ASCE, 118(3), 476–494.
De Vriend, M. (1973). "River bed variations—aggradation and degradation." *Pub. No. 107*, Delft Hydraulics Lab., Delft, The Netherlands.
Engelund, F., and Hansen, E. (1967). *A monograph on sediment transport in alluvial streams*. Danish Technical Press, Copenhagen, Denmark.
Gerald, C. F., and Wheatley, P. O. (1989). *Applied numerical analysis*, 4th Ed., Addison-Wesley Publishing Co., New York, N.Y.
Holly, F. M., and Rahuel, J. L. (1990). "New numerical/physical framework for mobile-bed modeling." *J. Hydr. Res.*, 28(4), 401–416.
Lai, C. (1991). "Modeling alluvial-channel flow by multimode characteristics method." *J. Engrg. Mech.*, ASCE, 117(1), 32–53.
Lai, C. (1994). "Multicomponent-flow analyses by multimode method of characteristics." *J. Hydr. Engrg.*, ASCE, 120(3), 378–395.
Rahuel, J. L., Holly, F. M., Chollet, J. P., Belleudy, P. J., and Yang, G. (1989). "Modeling of riverbed evolution for bedload sediment mixtures." *J. Hydr. Engrg.*, ASCE, 115(11), 1521–1542.
Wu, C. M. (1973). "Unsteady flow in open channel with movable bed." *Proc., Int. Symp. on River Mech.*, Int. Assoc. for Hydr. Res. (IAHR), Bangkok, Thailand, Vol. 3, 447–488.
Yang, J. C., Yeh, K. C., and Wu, C. M. (1992). "Numerical simulation of transient sediment laden flow in an alluvial channel." *Proc., 5th Int. Symp. on River Sedimentation*, Univ. of Karlsruhe, Karlsruhe, Germany, Vol. 1, 375–379.
Yeh, K. C., Wu, C. M., Yang, J. C., and Li, S. J. (1993). "Nonuniform transient sediment transport modeling." *Proc., 1993 Nat. Conf. on Hydr. Engrg.*, ASCE, New York, N.Y., Vol. 2, 893–898.

APPENDIX II. NOTATION

The following symbols are used in this paper:

A = flow area;
a = mixing-layer thickness;
a_j = component of eigenvector corresponding to given eigenvalue;
B = channel width;
C_f = correction factor of sediment-discharge formula;
$\mathbf{C}_j$ = column vector of $(N + 3)$ constants at section j;
$\mathbf{D}_j$, $\mathbf{L}_j$, $\mathbf{R}_j$ = coefficient matrices associated with $(N + 3)$ compatibility equations;
d_{si} = particle size of size class i;
d_{50}, d_m = median and mean particle sizes, respectively;
f_i = sediment transport capacity of d_{si};
g = gravitational acceleration;
h = flow depth;
L = number of subreaches of channel;
M = allowed maximum reachback number;
N = number of bed-material size fractions;
P_{bi}, P_{bio} = fractions of sediment in the ith size range in mixing layer and parent bed, respectively;
p_r = sediment porosity;
q_s = sediment transport capacity in volume per unit width;
S_f = friction slope;
s_g = specific gravity of sediment;
u = flow velocity;
$\mathbf{X}_j$ = column vector of $(N + 3)$ unknowns at section j;
z = bed elevation;
γ_s, γ = specific weights of sediment and water, respectively;
Δt = numerical time step;
Δx = numerical space step;
$\eta_{1,2}$ = spatial-interpolation factor;
θ = weighting factor;
λ_j = characteristic value or eigenvalue;
$\xi_{1,2}$ = temporal-interpolation factor; and
ϕ_j^{k+1} = general expression of unknowns at $x = j\Delta x$ and $t = (k + 1)\Delta t$.